J. Fluid Mech. (1976), *vol.* 74, *part* 1, *pp.* 59–79
Printed in Great Britain

Viscous boundary layers in reversing flow

By T. J. PEDLEY

Department of Applied Mathematics and Theoretical Physics,
University of Cambridge

(Received 15 September 1975)

The viscous boundary layer on a finite flat plate in a stream which reverses its direction once (at $t = 0$) is analysed using an improved version of the approximate method described earlier (Pedley 1975). Long before reversal ($t < -t_1$), the flow at a point on the plate will be quasi-steady; long after reversal ($t > t_2$), the flow will again be quasi-steady, but with the leading edge at the other end of the plate. In between ($-t_1 < t < t_2$) the flow is governed approximately by the diffusion equation, and we choose a simple solution of that equation which ensures that the displacement thickness of the boundary layer remains constant at $t = -t_1$. The results of the theory, in the form of the wall shear rate at a point as a function of time, are given both for a uniformly decelerating stream, and for a sinusoidally oscillating stream which reverses its direction twice every cycle. The theory is further modified to cover streams which do not reverse, but for which the quasi-steady solution breaks down because the velocity becomes very small. The analysis is also applied to predict the wall shear rate at the entrance to a straight pipe when the core velocity varies with time as in a dog's aorta. The results show positive and negative peak values of shear very much larger than the mean. They suggest that, if wall shear is implicated in the generation of atherosclerosis because it alters the permeability of the wall to large molecules, then an appropriate index of wall shear at a point is more likely to be the r.m.s. value than the mean.

1. Introduction

There are many situations in which fluid flows backwards and forwards past a solid boundary, or, equivalently, in which a boundary moves backwards and forwards in a steadily moving fluid. Examples include the motion induced by water waves on submerged bodies, the motion set up by a vibrating body in still fluid, and the flow of air past the wing of a hovering insect. One of the most important examples is to be found in the flow of blood in large arteries. Here the blood is pumped along by large amplitude pulsations of the heart, which generate large positive velocities (about 1·4 m s^{-1} in the human aorta) during the ejection phase followed by a marked flow reversal (minimum velocity about $-0{\cdot}4$ m s^{-1}) as the aortic valve closes, and a final recovery phase when the blood comes almost to rest (see figure 8 below). There are two reasons why it is important to understand the interaction of this reversing flow with a solid boundary.

(i) There is increasing evidence that the shear stress exerted by the blood on

the artery wall is an important factor in the generation of atherosclerotic lesions, which are one of the principal causes of circulatory failure. It is observed that lesions are distributed non-uniformly round the surface of arteries, more commonly being found near bifurcations, on the inner walls of curves, and in larger arteries rather than smaller ones (except near the entrance to the aorta, which is relatively free of lesions). The regions where lesions tend to develop are closely correlated both with areas of the wall in which the innermost cells (the *endothelial cells*) are found experimentally to have a relatively low permeability to large molecules, such as the lipoproteins which are known to be implicated in the generation of lesions, and with areas which would be expected to experience a relatively low wall shear, at least in steady flow. These observations have led to the linked pair of hypotheses (*a*) that lesions develop most readily in regions where the lipoproteins in the wall have difficulty getting out, and (*b*) that a relatively low level of shear stress reduces the permeability of endothelial cells. (The reader is referred to Lighthill (1975, chap. 13) for a more extensive discussion of the evidence, and to Caro (1973) and Fry (1973) for details of many of the relevant experiments.) There is still a long way to go before these hypotheses are fully verified, and even further before they are explained. In particular, very little is known about the mechanism by which wall shear stress affects endothelial permeability, apart from the fact that it has nothing to do with the greater thickness of the mass-transfer boundary layer in the blood in a region of low shear. If this were the controlling factor, the flux of material into or out of the wall would be far greater than that observed (Caro 1973). Thus it is not known whether it is the mean shear stress which is important as originally suggested (Caro, Fitz-Gerald & Schroter 1971), or some measure of the average level of shear stress experienced, such as the r.m.s. value. It is clear that one of the prerequisites for an understanding of the process is a knowledge of what the shear stress on the artery wall is, as a function of time, and how it changes from point to point. At the moment, experimental techniques are not adequate to measure the time-dependent shear stress on the wall of even a rigid cast of a large artery, because the boundary layers are very thin, and currently available methods do not have either fine enough resolution or good enough frequency response. Theoretical predictions are therefore needed, and one of the objectives of the present work is to develop a method for predicting the wall shear stress near the entrance of a large artery, in which the flow periodically reverses. The method is applied to the entrance of a dog's aorta in §4.

(ii) As well as flowing past the walls of blood vessels, the blood also flows past any object placed in a vessel. In recent years various methods have been developed for measuring blood velocity at a point in a large artery, in order to be able to plot velocity profiles and to describe the characteristics of any turbulence which may be present. The most successful such method so far has been that of hot-film anemometry, in which a small probe with a thin metal strip embedded in the surface is inserted into the artery. The velocity is inferred from measurements of the heat transfer from the strip when it is maintained at a fixed temperature above that of the blood (see Seed & Wood 1970; Clark 1974). The anemometer is calibrated for *in vivo* studies by placing the probe in a sequence of known steady

flows, and assuming that its response in an unsteady flow is quasi-steady. Laboratory studies in known oscillatory flows have shown that this is a good assumption for the probes used, except for a period around the time when the flow reverses its direction and the blood velocity is low. The behaviour of such a probe in non-reversing oscillatory flow was examined theoretically in two earlier papers (Pedley 1972*a*, *b*), in which (*a*) the thermal boundary layer on the hot film (and hence the heat transfer) was analysed on the assumption that the unsteady wall shear rate on the probe was known, and (*b*) this wall shear rate was predicted from a study of the viscous boundary layer on the probe, driven by the oscillatory free stream. Many idealizations were introduced in the theoretical model (for example that the velocity and temperature fields are two-dimensional), but the most restrictive was the requirement that not only the free stream but also the wall shear rate over the film should not reverse its direction. This meant that the departure from quasi-steady behaviour became significant only after the theory was no longer applicable, and one of the objects of the present work is to extend the theory to cover reversing flow. A simple model of the probe is that of a finite flat plate with a heated film on the surface near its mid-point. The variation of wall shear rate on a finite flat plate in a reversing free stream is computed in §§2 and 3 of this paper. The rate of heat transfer from the hot film, driven by the oscillatory wall shear rate, will be the subject of a future paper.

Throughout this paper we shall treat the motion of a homogeneous Newtonian fluid of kinematic viscosity ν. In the applications to blood flow, therefore, we explicitly assume that the non-Newtonian and non-homogeneous properties of blood (which is a concentrated suspension of flexible red cells) can be ignored. This is justified as long as the shear rates in the fluid do not fall below $100\ \mathrm{s}^{-1}$, and so long as the length scales of the flow are large compared with the cell diameter and spacing, which are of the order of $10\ \mu\mathrm{m}$ (see Whitmore 1968, Chap. 6). The kinematic viscosity of whole blood is normally about $4 \times 10^{-6}\ \mathrm{m}^2\ \mathrm{s}^{-1}$.

The ideas behind the approximate method used here to analyse boundary layers in reversing flow were outlined in a recent paper (Pedley 1975). In it the method was applied to a very simple thermal boundary-layer problem to which an exact solution was available so that the accuracy of the approximate method could be assessed. It was found to be quite acceptable: the maximum error in the prediction of the heat transfer from a heated strip in a uniform reversing flow was less than 17%. In the next section the application of the method to two-dimensional viscous boundary layers is explained fully, and a modification introduced which is expected to increase the accuracy still further.

2. Development of the approximate theory

Consider a finite flat plate occupying the region $0 \leqslant \hat{x} \leqslant L$ of the plane $\hat{y} = 0$ with velocity $\hat{U}(\hat{t})$ in the $\hat{x}$ direction far from the plate, varying with characteristic frequency ω. Suppose that the flow reverses its direction once, at $\hat{t} = 0$, and that $\hat{U} \gtrless 0$ for $\hat{t} \lessgtr 0$. Suppose too that, long before $\hat{t} = 0$, the Reynolds number $L\hat{U}(\hat{t})/\nu$ is large, and the frequency parameter $\omega L/\hat{U}(\hat{t})$ is small. There will then be an approximately quasi-steady boundary layer on the plate, growing from

the leading edge $\hat{x} = 0$. (There will also be a quasi-steady wake downstream, and small regions of length scale $\nu/\hat{U}(\hat{t})$ near the leading and trailing edges where boundary-layer theory is not applicable, but these regions will be ignored.) Similarly, long after $\hat{t} = 0$, there will be a quasi-steady boundary layer growing from the new leading edge $\hat{x} = L$, as long as the Reynolds number and frequency parameter are again large and small respectively.

We introduce dimensionless variables as follows:

$$x = \hat{x}/L, \quad y = \hat{y}(U_0/\nu L)^{\frac{1}{2}}, \quad t = \hat{t}U_0/L, \quad u = \hat{u}/U_0, \quad U = \hat{U}/U_0,$$

where U_0 is an appropriate velocity scale for the free-stream velocity $\hat{U}(\hat{t})$. The boundary-layer equation governing the x component of velocity, $u(x, y, t)$, over the flat plate is now

$$(u_t - U_t) + \left(uu_x - u_y \int_0^y u_x dy\right) = u_{yy}, \tag{1}$$

with boundary conditions

$$u = 0 \quad \text{on} \quad y = 0, \qquad u \to U(t) \quad \text{as} \quad y \to \infty. \tag{2}$$

The flow in the quasi-steady boundary layers represents a balance between the convective inertia terms in (1) (the second bracket on the left-hand side) and the viscous term (the right-hand side). The velocity profile in each case is the familiar Blasius profile; for example, when $t < 0$, we have

$$u = U(t)f'(\eta_1), \quad \text{where} \quad \eta_1 = y[U(t)/2x]^{\frac{1}{2}}, \tag{3}$$

and $f(\eta_1)$ is the solution of

$$f''' + ff'' = 0, \quad f(0) = f'(0) = 0, \quad f'(\infty) = 1.$$

This quasi-steady solution remains accurate as long as the unsteady inertia terms, the first bracket on the left-hand side of (1), are small compared with the convective terms, i.e. as long as

$$\epsilon_1 \equiv x|\dot{U}|/U^2 \ll 1, \tag{4}$$

where $\dot{U} = dU/dt$. As t approaches zero, however, U becomes very small, and ϵ_1 becomes very large (unless $\dot{U}$ is also zero at $t = 0$). This suggests that, near $t = 0$, the flow will be approximately represented by a diffusive balance between the unsteady inertia terms and the viscous term. Vorticity will continue to diffuse out into the fluid until convection once more becomes important as the flow is accelerated in the opposite direction. The boundary-layer approximation is still expected to be applicable to the diffusive flow as long as there is not enough time for the layer thickness to become comparable with L before the new quasi-steady boundary layer takes over.

The approximate solution for u throughout the period of reversal is constructed by asserting that at every point x on the flat plate the flow is initially quasi-steady, and approximately given by (3). Then, at a definite time $t = -t_1(x) < 0$, there is an abrupt, instead of a gradual, transition to a diffusive solution, obtained from (1) without the second bracket. Then at another definite time $t = +t_2(x) > 0$, the new quasi-steady boundary layer, growing from $x = 1$,

takes over. The solution in the periods of approximately quasi-steady flow can be made more accurate by including the second term in an expansion in which the unsteady inertia terms are taken to be first-order small quantities; for $t < 0$ this second term is $O(\epsilon_1)$. Pedley (1972*b*) showed that the first two terms of this expansion are quite accurate as long as $\epsilon_1 \lesssim 0{\cdot}5$. Thus the full approximate solution for u is

$$u = U(t)\,[f'(\eta_1) + x\dot{U}U^{-2}f_1'(\eta_1)] \quad \text{for} \quad t \leqslant -t_1(x), \tag{5}$$

where η_1 is given by (3);

$$u = U(t)\,[f'(\eta_2) - (1-x)\,\dot{U}U^{-2}f_1'(\eta_2)] \quad \text{for} \quad t \geqslant t_2(x), \tag{6}$$

where

$$\eta_2 = y[-U(t)/2(1-x)]^{\frac{1}{2}};$$

$$u = U(t) - 2\pi^{-\frac{1}{2}}\int_{\eta_0}^{\infty} U\left[t - \frac{\eta_0^2(t+t_0)}{\mu^2}\right]e^{-\mu^2}\,d\mu \quad \text{for} \quad -t_1(x) < t < t_2(x), \tag{7}$$

where

$$\eta_0 = \tfrac{1}{2}y(t+t_0)^{-\frac{1}{2}}.$$

The function $f_1(\eta)$ appearing in (5) and (6) is the solution of

$$f_1''' + ff_1'' - 2f'f_1' + 3f''f_1 = \eta f'' + 2f' - 2,$$
$$f_1(0) = f_1'(0) = f_1'(\infty) = 0,$$

which was first solved by Moore (1951). Equations (5) and (6) give the improved quasi-steady boundary-layer profiles, expected to be accurate as long as $\epsilon_1 \lesssim 0{\cdot}5$ and

$$\epsilon_2 = (1-x)\,|\dot{U}|/U^2 \lesssim 0{\cdot}5 \tag{8}$$

respectively. Equation (7) gives the solution of the diffusion equation (equation (1) without the convective inertia terms) which satisfies the initial condition

$$u = 0 \quad \text{at} \quad t = -t_0(x)$$

as well as the boundary conditions (2). All that is now required is to evaluate the unknown functions $t_1(x)$, $t_2(x)$ and $t_0(x)$.

The quantities t_1 and t_2 are determined in the same way as in Pedley (1975). The influence of the leading edge cannot be felt at a point x unless fluid particles which have passed the leading edge arrive at that point. We therefore assert that the diffusive solution takes over from the initial quasi-steady solution at a time $(-t_1)$ when fluid particles which pass the leading edge ($x = 0$) at that time just fail to reach the point x before flow reversal at $t = 0$. Thus t_1 is given by

$$x = \int_{-t_1(x)}^{0} U(t)\,dt. \tag{9}$$

Similarly, the new quasi-steady solution, which develops when $t > 0$ from the new leading edge $x = 1$, will take over from the diffusive solution at a time (t_2) when fluid particles which have passed $x = 1$ first reach the point. Hence

$$1 - x = -\int_{0}^{t_2(x)} U(t)\,dt. \tag{10}$$

This method of evaluating t_1 and t_2 is consistent with the solutions which have been obtained for the classic problem of the impulsively-started flat plate with

leading edge at $x = 0$ ($U = 0, t \leqslant 0$; $U = 1, t > 0$; thus $t_2 \equiv x$). Stewartson (1973) has shown how information about the leading edge is convected along at the outer edge of the boundary layer with the free-stream velocity, but is simultaneously transmitted to the inner parts of the layer by diffusion. Thus the whole boundary layer is influenced by the leading edge when $t > x$. Numerical calculations of the wall shear rate do not show any departure from the diffusive (Rayleigh) solution until $t > 1{\cdot}5x$ (Hall 1969; Dennis 1972), but Stewartson (1973) quotes numerical predictions of the displacement thickness which depart significantly from diffusive values for $t > 1{\cdot}1x$. Thus equations (9) and (10) give values of t_1 and t_2 which may be slightly below the 'best' estimate from the numerical point of view, but it is not clear how to improve them. Alternatively it may be possible to choose $-t_1$ and t_2 as those values of t for which ϵ_1 (equation (4)) and ϵ_2 (equation (8)) are respectively equal to 0·5. As we shall see, the latter choice yields results which are closely comparable with those obtained from the former, and we believe that (9) and (10) are not sources of great inaccuracy.

At $t = -t_1$, the diffusive solution (7) takes over from the quasi-steady solution (5). The only disposable parameter which can still be adjusted to take account of the velocity field which is present before the take-over is $t_0(x)$. Ideally, the velocity field would be continuous at $t = -t_1$; in the simple problem discussed by Pedley (1975) the temperature field could be made continuous by a suitable choice of t_0. Here, however, this is not possible because the shapes of the quasi-steady and the diffusive velocity profiles are different. Of course, it would be possible to solve the diffusion equation with an initial profile given by (5) at $t = -t_1$, but then the simplicity of the solution (7) would be lost, and the whole theory could become extremely cumbersome. Therefore, t_0 must be chosen such that some index of the velocity field is continuous. We take that index to be the displacement thickness of the layer, δ_1, defined by

$$U\delta_1 = \int_0^\infty (U - u)\, dy. \tag{11}$$

This seems the best choice because $U\delta_1$ is proportional to the mass flux deficit in the boundary layer, and if it is not made continuous then conservation of mass, the most fundamental of all conserved quantities, is not preserved. This choice of course means that other quantities, like the dimensionless wall shear rate τ ($= [-\partial u/\partial y]_{y=0}$, proportional to the skin friction) and the momentum thickness δ_2, are not continuous at $t = -t_1$. It is sometimes argued that the momentum thickness should always be continuous, at least in steady flow, because a jump in δ_2 means a locally infinite value of τ, from the integral form of the momentum equation:

$$U^2 \frac{\partial \delta_2}{\partial x} + \frac{\partial}{\partial t}(U\delta_1) = \tau \tag{12}$$

(Rosenhead 1963, p. 207). Since the object of the theory is to calculate τ, it might be better to make δ_2 or even τ itself continuous. However, in unsteady flow, a jump in δ_1 would also lead to a singularity in τ, from (12), and in any case it is possible to exclude the singularity from predictions of τ. Furthermore, although making τ continuous would make the results look smoother, there

would be no guarantee that they were more correct. It is shown below in a particular example that the difference in the predictions of τ obtained by taking δ_1 and δ_2 continuous is very small; δ_1 is also easier to compute. For all these reasons, therefore, the choice of δ_1 as the continuous quantity seems well justified. Continuity of δ_1 at $t = -t_1(x)$ leads to the following equation for $t_0(x)$, derived from (5), (7) and (11):

$$[2xU(-t_1)]^{\frac{1}{2}}\left[\delta_{10}-\frac{x\dot{U}(-t_1)}{U^2(-t_1)}\delta_{11}\right] = 2\left(\frac{t_0-t_1}{\pi}\right)^{\frac{1}{2}}\int_0^1 U[-t_1-\lambda^2(t_0-t_1)]\,d\lambda, \quad (13)$$

where

$$\delta_{10} = \int_0^\infty [1-f'(\eta)]\,d\eta = 1{\cdot}217,$$

$$\delta_{11} = f_1(\infty) = 0{\cdot}727.$$

All quantities appearing in the solution have now been determined. It will be seen that even δ_1 will be discontinuous at $t = +t_2$, when the new quasi-steady boundary layer takes over from the diffusing solution. This is to be expected, because the boundary-layer equations are parabolic in x, and the new quasi-steady layer, growing from $x = 1$, can be influenced only by upstream conditions, at smaller values of $1-x$. It cannot depend on the flow from which it takes over. In practice, continuity of the velocity field would be achieved by the presence of eigenfunctions, like those examined by Stewartson (1973) and by Watson in the appendix to Dennis (1972). These are so complicated, however, that they would destroy the simplicity of the present method; we must accept the possibility of inaccuracy for times close to $t_2(x)$.

The results of the theory will be presented in terms of the dimensionless shear rate at the wall, $\tau(x,t)$. This is given by

$$\tau = \begin{cases} \dfrac{[U(t)]^{\frac{3}{2}}}{(2x)^{\frac{1}{2}}}\left[f''(0)+\dfrac{x\dot{U}(t)}{U^2(t)}f_1''(0)\right] & \text{for } t \leqslant -t_1, \quad (14a) \\ U(t)\left[\dfrac{-U(t)}{2(1-x)}\right]^{\frac{1}{2}}\left[f''(0)-\dfrac{(1-x)\dot{U}(t)}{U^2(t)}f_1''(0)\right] & \text{for } t \geqslant t_2, \quad (14b) \\ 2\pi^{-\frac{1}{2}}\left\{U(-t_0)+2(t+t_0)\displaystyle\int_0^1 \dot{U}[t-\lambda^2(t+t_0)]\,d\lambda\right\} & \text{for } -t_1 < t < t_2, \quad (14c) \end{cases}$$

where

$$f''(0) = 0{\cdot}470, \quad f_1''(0) = 1{\cdot}200.$$

Approximate methods have been used previously to analyse unsteady boundary layers, although they have all required the use of rather cumbersome integral transform techniques, and could not be readily adapted to cover a wide range of actual problems. Atabek & Chang (1961), in a discussion of unsteady entry flow in a tube (applied to the aorta, as in §4 here), used the Oseen approximation, replacing the convective inertia terms in (1) by Uu_x. This made the equation linear, and therefore relatively easy to solve. However, while this might be expected to give an accurate description of the flow at the outer edge of the boundary layer, there are no grounds for supposing it to be a good approximation near the wall, where $u \ll U$ and where the shear stress is calculated. The present method is certainly much more accurate in the quasi-steady regimes

($t < -t_1$ and $t > t_2$), it is unlikely to be more inaccurate during the intermediate period when U is small, and it is easier to use. A modified Oseen approximation was proposed by Lewis & Carrier (1949), who replaced the convective inertia terms by cUu_x, for some constant c such that $0 < c < 1$. The quantity cU was to represent an average across the boundary layer of the convection velocity. These authors found that if c was taken equal to 0·35, a value of τ equal to the Blasius value was obtained for steady flow over a flat plate. Carrier & DiPrima (1956) subsequently applied the method to small amplitude oscillatory flow over a semi-infinite flat plate; it has the merit of giving the correct answer in steady flow, and of predicting a continuous velocity field. However, it has not been used for large amplitude oscillations, and there is no way of knowing whether a constant value of c is appropriate throughout a flow reversal, or for different geometries (e.g. with an x-dependent outer flow). The present method is preferred because it is less cumbersome, it is more generally applicable, and it is known to be accurate during the quasi-steady regimes.

3. Results for the finite flat plate

The first time-varying motion to be considered is the simplest one in which the outer flow reverses smoothly at $t = 0$, i.e. it is the uniform deceleration

$$\hat{U} = -A\hat{t} \quad \text{or} \quad U = -t;$$

the velocity scale U_0 is here replaced by $(AL)^{\frac{1}{2}}$. Application of the approximate method is very straightforward, because (9) and (10) can be solved explicitly, yielding

$$t_1 = (2x)^{\frac{1}{2}}, \quad t_2 = [2(1-x)]^{\frac{1}{2}},$$

and (13) reduces to a simple cubic equation for t_0. We may note that in this case ϵ_1 and ϵ_2 ((4) and (8)) are identically equal to $\frac{1}{2}$ when $t = -t_1$ and $+t_2$ respectively, so that the two alternative methods of choosing t_1 and t_2 yield the same results. We examine this simple flow in order to answer two questions. (*a*) Is it worth including the modification to the quasi-steady solutions, represented by the second term in the square brackets of (5) and (6)? (*b*) Does the different value of t_0 derived from continuity of momentum thickness rather than displacement thickness significantly alter the predictions of wall shear?

The dimensionless wall shear rate τ, derived from (14) and evaluated at the mid-point of the plate, $x = 0{\cdot}5$ (so that $t_1 = t_2 = 1$), is plotted against t in figure 1(*a*). The full curve was obtained using the modified quasi-steady solution, while the broken curve was obtained from the simple quasi-steady solution, in which δ_{11} in (13) and $f_1''(0)$ in (14) were set equal to zero (a completely quasi-steady curve would pass through the origin, joining up the outer parts of the broken curve). We can see that the modified solution is significantly different, especially for $t < -t_1$ and $t > t_2$, where it is known to be more accurate. The shear stress reverses its sign before the outer flow, because the slower-moving fluid near the wall responds more readily to the applied adverse pressure gradient (proportional

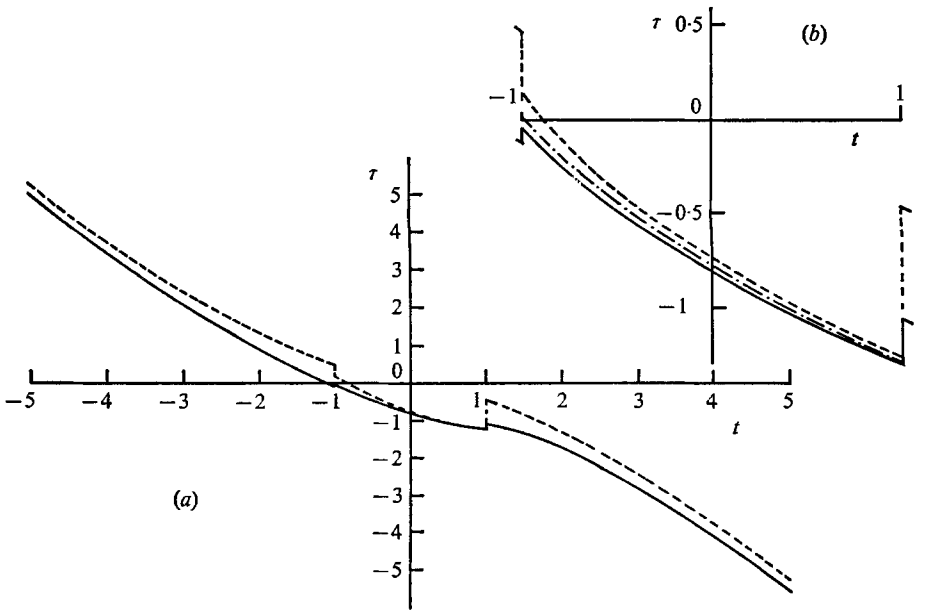

FIGURE 1. (*a*) Dimensionless wall shear rate at the mid-point of the plate ($x = 0{\cdot}5$) plotted against time during a uniform deceleration of the flow. ———, approximate solution using modified quasi-steady solution; – – –, approximate solution using unmodified quasi-steady solution. (*b*) Enlarged version of the central part of (*a*), including the solution derived from continuity of momentum thickness, not displacement thickness, at $t = -t_1$ (dash–dot curve).

to $\dot{U}$) than does the free stream. Note that the diffusive solution gives an overestimate of the magnitude of the wall shear at the end of the diffusive phase; this is a consistent feature of all the results so far obtained. We see too that the modified solution effectively eliminates the discontinuity in τ at $t = -t_1$, and the discontinuity at $t = t_2$ is also much reduced. It is therefore worth including the modification. The central region of figure 1(*a*), where the diffusive solution is in force, is shown on an enlarged scale in figure 1(*b*), and the graph obtained with continuity of momentum thickness rather than displacement thickness is included as the dash–dot curve. It can be seen to give results differing by a small amount, which is greatest for times close to $-t_1$, where the (small) discontinuity in τ is doubled, and least for times close to t_2, where the discontinuity is fractionally reduced. The use of displacement thickness is therefore vindicated.

Calibration experiments in which hot-film anemometers have been tested in unsteady flows have used sinusoidal oscillations in the stream velocity (Seed & Wood 1970; Clark 1974). These are also the simplest type of oscillation to assess theoretically. We therefore apply the present theory to a flow for which

$$U = 1 + \alpha \cos \omega t. \tag{15}$$

Since we are primarily interested in flows which reverse their direction, we shall mostly consider values of the amplitude parameter α greater than one. U is

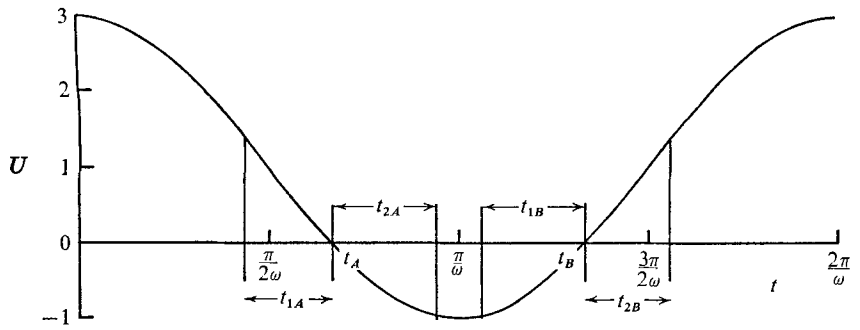

FIGURE 2. Sinusoidal velocity $U(t)$ given by (15), for the case $\alpha = 2{\cdot}0$. Times of flow reversal are $t = t_A, t_B$. Values of $t_{1A,B}$ and $t_{2A,B}$ are also plotted for the case $\omega = 1{\cdot}0$, $x = 0{\cdot}5$.

plotted in figure 2 for the case $\alpha = 2$. Note that the times of flow reversal are not $t = 0$, but $t = t_A$ and $t = t_B$, where

$$t_A = 2\pi - t_B = \omega^{-1}[\pi - \cos^{-1}(\alpha^{-1})];$$

hence the origin of time in the analysis of § 2 is shifted. Also marked on figure 2 are typical values of t_1 and t_2 for each each flow reversal ($t_{1A,B}$ and $t_{2A,B}$); they are the values for $\omega = 1{\cdot}0$ and $x = 0{\cdot}5$.

We also restrict attention to situations for which there is a quasi-steady regime at the beginning and end of each cycle, near the time of maximum forward velocity. This means that the frequency of the oscillation must be sufficiently small that fluid particles which have passed the leading edge $x = 0$ do reach the point x during the same cycle. It is therefore necessary that $t_{1A}(x)$ is smaller than t_A, and hence that

$$\omega(x - t_A) < (\alpha^2 - 1)^{\frac{1}{2}}. \tag{16}$$

What happens when this requirement is not satisfied is discussed in the next section. Note that the frequency parameter ω is equal to $\Omega L/U_0$, where Ω is the angular frequency of the oscillation.

The theory can be applied whether or not a reversed quasi-steady boundary layer appears, growing from the new leading edge at $x = 1$, i.e. whether or not ωt_{2A} is less than $\pi - \omega t_A$. The requirement for the reversed quasi-steady solution to arrive at a point x is that

$$\omega(1 - x - t_A) < (\alpha^2 - 1)^{\frac{1}{2}} - \pi. \tag{17}$$

If this is not satisfied, the diffusive solution must be used throughout the region of reversed flow, not giving way to another quasi-steady regime until after the second reversal in U, at $t = t_{2B}$, when the quasi-steady boundary layer has once more grown from $x = 0$.

Thus when $\alpha > 1$, the computational procedure at each x is as follows.

(i) Check that (16) is satisfied, so that a quasi-steady regime exists at $t = 0$.

(ii) Calculate $t_{1A}(x)$, using (9) with time origin shifted to t_A; this computation is done iteratively.

(iii) Check whether (17) is satisfied.

(iv) If so, compute $t_{2A}(x)$ from (10) (again with origin at t_A), and then $t_{1B}(x)$ from (9) with origin at t_B (for this sinusoidal example $t_{1B} = t_{2A}$); if not, go straight to (v).

(v) Compute $t_{2B}(x)$ from (10) with origin at t_B (for this sinusoidal example $t_{2B} = t_{1A}$).

(vi) Calculate the values of ϵ_1 or ϵ_2 ((4) and (8)) at each take-over time, to see whether they are close to 0·5.

(vii) Compute t_0 for the first reversal from (13) with origin at t_A; this will again require an iterative solution.

(viii) Repeat for the second reversal, if t_{1B} exists. Even when it does, it sometimes happens that $\omega(t_B - t_{1B})$ is so close to $\frac{1}{2}\pi$ that (13) does not have a solution. In this case we choose the value of t_{0B} so as to minimize the difference between the two sides of that equation; that value turns out to be equal to $t_B - t_A$.

(ix) Compute the wall shear rate as a function of time from (14). The integrals in (13) and (14*c*) would normally have to be evaluated numerically; in this case they can be expressed in terms of the Fresnel integrals

$$C(z) = \int_0^z \cos(\tfrac{1}{2}\pi t^2)\,dt, \quad S(z) = \int_0^z \sin(\tfrac{1}{2}\pi t^2)\,dt,$$

which are tabulated and can therefore be used as a check.

Before presenting numerical results, we note that the theory can also be adapted for cases in which the outer flow does not reverse ($\alpha < 1$), but in which the modified quasi-steady solution breaks down because U becomes small near the time of minimum velocity. In such cases our usual criteria for calculating the times at which the diffusive solution should be used cannot be applied. We therefore assert that the diffusive solution takes over from the (modified) quasi-steady solution at the time, $\pi/\omega - t_1(x)$, when ϵ_1 [equation (4)] first equals 0·5 and is increasing. (There is also a time very close to π/ω at which $\epsilon_1 = 0{\cdot}5$ and is decreasing, because $\dot{U} = 0$ at $t = \pi/\omega$.) A new quasi-steady solution will take over at $t = \pi/\omega + t_1(x)$. If ϵ_1 is always less than 0·5, the (modified) quasi-steady solution is valid at all times.

In the hot-film calibration experiments of Seed & Wood (1970) the value of α ranged from about 0·5 to about 5·0, and the value of ω from zero to about 3·0; x was about 0·5. In Clark's (1974) experiments, α was always taken to be less than 1 (maximum value 0·84), but ωx reached values of up to 30, at which any theory incorporating quasi-steady boundary layers would be inappropriate. Here we illustrate the results of the theory with two values of α, one greater than 1 (= 2·0) and one slightly less than 1 (= 0·98, a particular value used by Seed & Wood). Most of the results quoted are for $x = 0{\cdot}5$, because the hot film in both sets of experiments lay near the centre of the probe, i.e. of the finite flat plate. In the case $\alpha = 2{\cdot}0$, we use three values of the frequency parameter ω, equal to 0·1, 1·0 and 5·0 (note that the restriction (16) means that ω must be less than about 7·6 for the theory to be applicable with $\alpha = 2$ and $x = 0{\cdot}5$). In the case $\alpha = 0{\cdot}98$, we use only $\omega = 1{\cdot}0$.

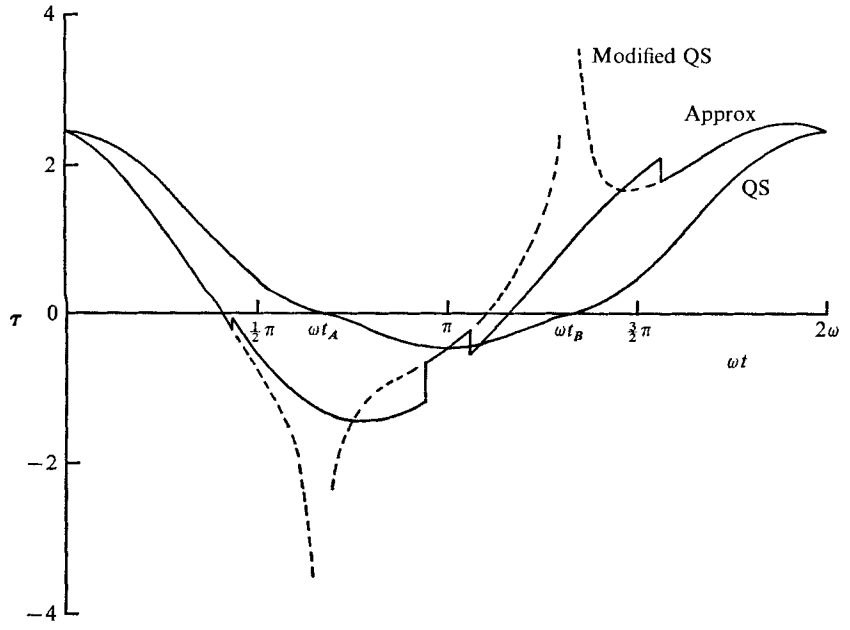

FIGURE 3. Dimensionless wall shear rate τ plotted against ωt for the case $\alpha = 2{\cdot}0$, $x = 0{\cdot}5$, $\omega = 1{\cdot}0$. Solid curves are the quasi-steady solution (QS) and the approximate solution obtained from the methods of this paper. The broken curve is the modified quasi-steady solution, singular at points of flow reversal.

In figure 3 the graph of τ against ωt is plotted for $\alpha = 2{\cdot}0$, $x = 0{\cdot}5$ and $\omega = 1{\cdot}0$. The curve marked QS was obtained from a completely quasi-steady analysis. The other solid curve was obtained using the approximate theory of this paper. The steps in the curve show that it is by no means perfect, but it is clearly an improvement, because it predicts both a phase lead of the wall shear over the stream velocity, and a greater amplitude of wall shear than would be predicted by quasi-steady theory. These are features of all such oscillatory flows, reaching an extreme in the high frequency limit, when the mean and the oscillatory flow are uncoupled. The former is then a Blasius boundary layer, and the latter is a Stokes layer; the wall shear oscillations have an amplitude which exceeds the mean by a factor of order $\alpha(\omega x)^{\frac{1}{2}}$ (see Pedley 1972*b*), and have a phase lead of $\frac{1}{4}\pi$ over the quasi-steady solution. The dangers of using the modified quasi-steady solution at all times are also illustrated in figure 3, by the broken curve. This becomes infinite when the stream velocity is zero, because of the factor $1/U^2$ in the second term inside the square brackets of equations (14) (i.e. ϵ_1 and ϵ_2 become infinite).

The effect of varying ω is shown in figure 4, where the curves of τ against ωt are again plotted for $\alpha = 2{\cdot}0$ and $x = 0{\cdot}5$, with $\omega = 0{\cdot}1$, $1{\cdot}0$ and $5{\cdot}0$. The low frequency curve ($\omega = 0{\cdot}1$) is not very different from the quasi-steady curve of figure 3, except that it shows reversal in wall shear significantly before the reversal in flow velocity. The discontinuities at the start of each diffusive phase are undetectable; the steps in the curve at the end of each such phase, at

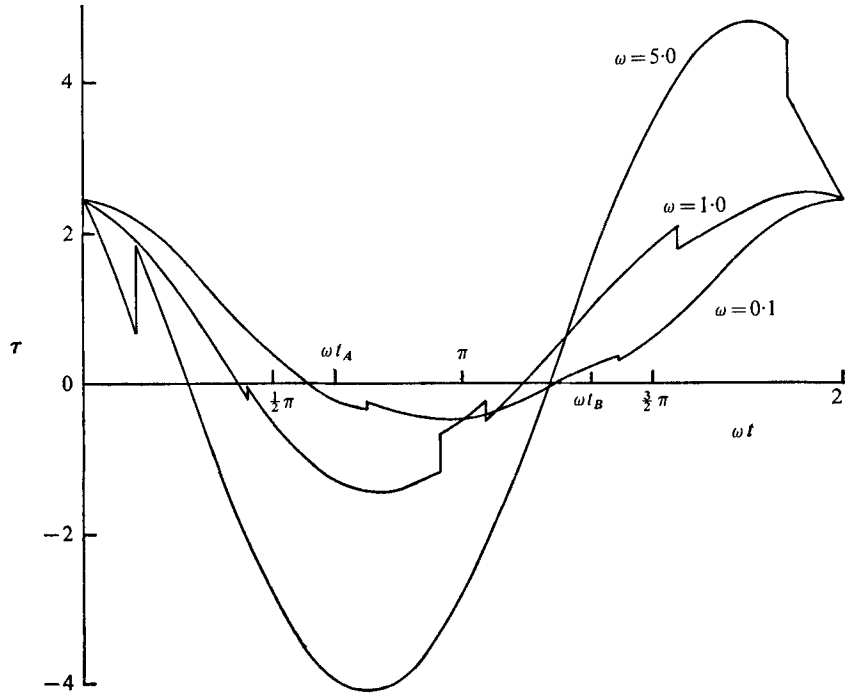

FIGURE 4. Graphs of τ against ωt for different values of ω, when $\alpha = 2{\cdot}0$, $x = 0{\cdot}5$.

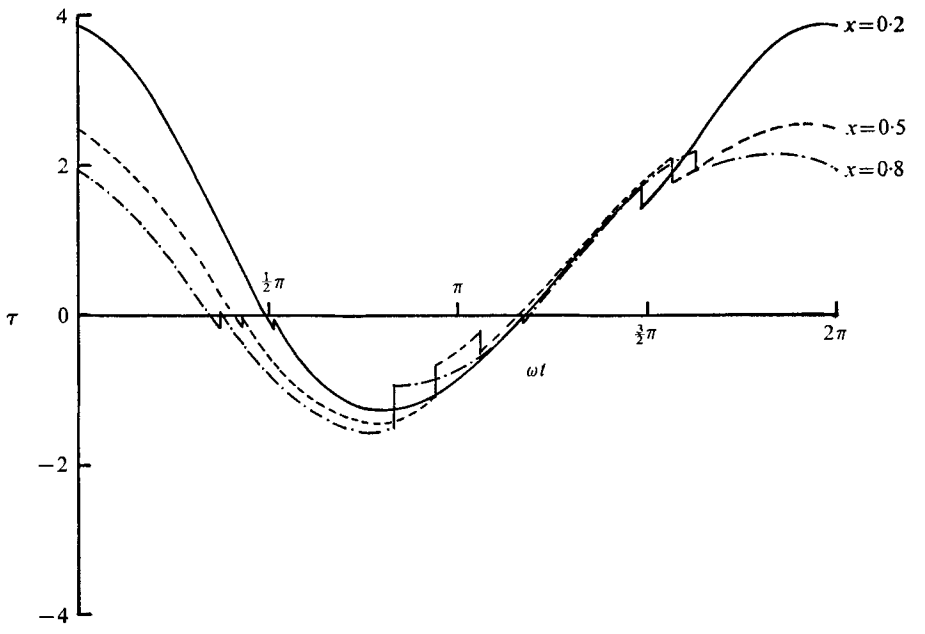

FIGURE 5. Graphs of τ against ωt for different values of x, when $\alpha = 2{\cdot}0$, $\omega = 1{\cdot}0$.

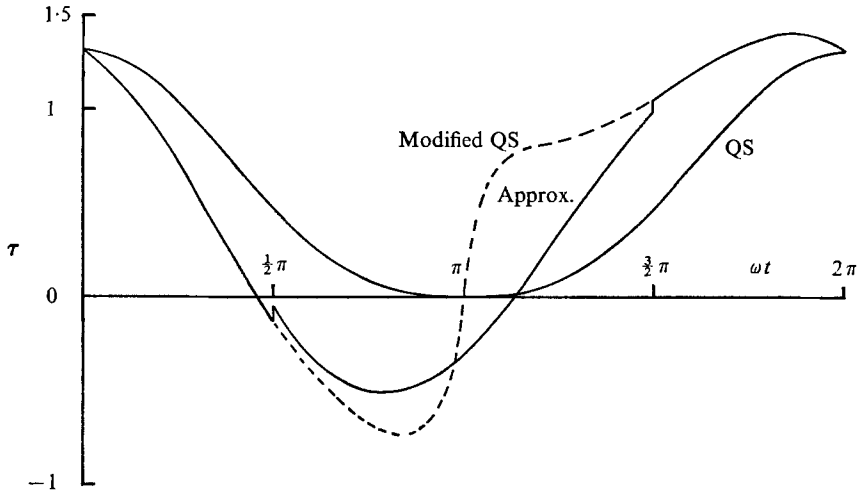

FIGURE 6. Graphs of τ against ωt for the case $\alpha = 0{\cdot}98$, $x = 0{\cdot}5$, $\omega = 1{\cdot}0$. Solid curves are the quasi-steady solution (QS) and the approximate solution obtained from the methods of this paper. The broken curve is the modified quasi-steady solution.

$t = t_A + t_{2A}$ and $t = t_B + t_{2B}$ are also very small. The curve for $\omega = 5{\cdot}0$ shows a dramatic increase in amplitude over that for $\omega = 1{\cdot}0$, by a factor of about 2·2. This is close to $\sqrt{5}$, the value predicted by Stokes-layer theory. Also the phase lead over the quasi-steady curve is almost exactly $\frac{1}{4}\pi$. There is still a short period, near the time of peak forward velocity, when the modified quasi-steady solution is expected to be appropriate, but this value of ω is close to the limit of applicability of the present theory.

The differences in the wall shear oscillations at different positions on the plate are shown in figure 5, where curves are plotted for $\alpha = 2{\cdot}0$, $\omega = 1{\cdot}0$ and $x = 0{\cdot}2$, $0{\cdot}5$ and $0{\cdot}8$. The greatest shear rates are predicted for $x = 0{\cdot}2$, because this point is nearest to the leading edge during the time of peak forward velocity. The reversed quasi-steady boundary layer, growing from $x = 1$, does not reach $x = 0{\cdot}2$ at any stage during the cycle, so the diffusive solution is taken throughout the reversed phase of the flow. This is not the case at $x = 0{\cdot}5$ and $0{\cdot}8$, which each briefly experience the reversed quasi-steady layer. However, the tendency of the diffusive solution to overestimate the magnitude of the wall shear at the end of the diffusive phase partially masks the fact that, during reversal, the point nearest $x = 1$ experiences the greatest wall shear. Results computed for $\alpha = 10$ show this feature clearly, but we do not plot them because they otherwise are qualitatively the same. It is very interesting that the wall shear at all three points is virtually the same during the second diffusive phase, near the second reversal in stream velocity. This indicates that, at this stage in the cycle, the flow almost everywhere on the plate resembles a Stokes layer, independent of the ends of the plate.

In every case for which computations have been made, the values of ϵ_1 and ϵ_2 have been calculated at the times of transition between the quasi-steady regime and the diffusive regime near the first zero, t_A, of U. The computations

covered values of α equal to 1·2 and 10·0 as well as 2·0, values of ω equal to 0·1, 1·0, 5·0 and 10·0, and values of x equal to 0·2, 0·5 and 0·8. In every case, except those for which $\alpha = \omega = 10{\cdot}0$, ϵ_1 lay in the range of 0·47 to 0·55; in the exceptional cases it took smaller values. Thus to choose $\epsilon_1 = 0{\cdot}5$ as the criterion of take-over in the case where the flow does not reverse seems well justified. The values of ϵ_2 were commonly smaller than 0·5, presumably because in many cases $t_A + t_{2A}$ was close to $\pi/2\omega$, so that $\dot{U}$ was small.

The results for $\alpha = 0{\cdot}98$, $\omega = 1{\cdot}0$ and $x = 0{\cdot}5$ are plotted in figure 6, together with the corresponding quasi-steady and modified quasi-steady curves (cf. figure 3). The phase lead and the increase in amplitude over the quasi-steady curve are again in evidence: the wall shear becomes negative near the time of minimum velocity, and the maximum negative shear is as much as 35% of the maximum positive shear.

4. Wall shear in the entrance to the aorta

The aorta is an elastic tube which stems from the left ventricle of the heart, and almost immediately curves in a complicated three-dimensional way through 180°, giving off branches to the head and upper limbs (figure 7). It then pursues a fairly straight course down in front of the spine, and the blood is distributed to the chest muscles, the abdominal organs and the lower limbs by means of further branches. In this paper we model the aorta as a straight, uniform, rigid tube. Thus many drastic simplifications are made, so that we can isolate the effect of unsteady flow without the complicating features of the real aorta. Nevertheless the results are still expected to be applicable in the short length of almost straight tube immediately downstream of the aortic valve (the 'ascending aorta') because most of the simplifications are justified there, as we discuss below.

(i) *Elasticity.* The elasticity of the vessel wall is important in determining how the pulse wave propagates, and hence in determining the local pressure gradient (proportional to $\dot{U}$) as a function of time. However, the flow which is driven by that pressure gradient is not greatly affected by the elasticity. This is because the wavelength of the wave (several metres in dog and man) is large compared with the distance travelled by a fluid element during one cycle (less than 10 cm). Thus to any fluid element, the tube appears to have parallel walls, although it varies in diameter by a few per cent during each beat. A similar argument shows that the taper of the real aorta is also unimportant.

(ii) *Branches.* The branches from the arch of the aorta will clearly have a significant influence on the flow near their entrances. However, their effect on the flow nearer to the heart is likely to be less pronounced. Measurements of velocity profiles in this region of the canine aorta show skews which can be fully accounted for by the curvature of the vessel (Nerem, Seed & Wood 1972). Very near to the heart another skew is introduced at certain times in the cycle, probably as a result of flow into the coronary arteries, which come off the widened part of the aorta just behind the valves.

(iii) *Curvature.* It is clear from the quoted measurements that curvature has

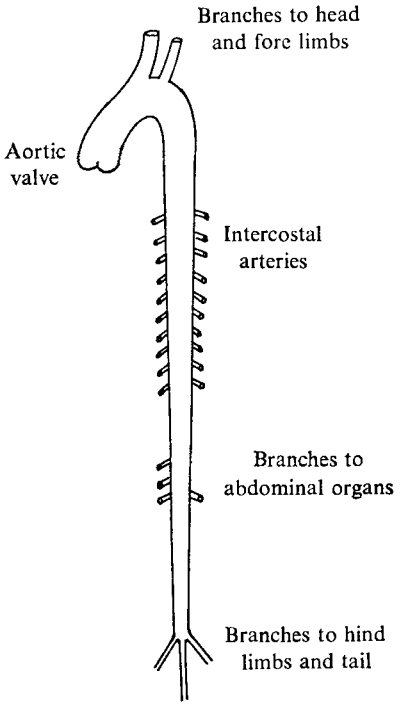

FIGURE 7. Sketch of the canine aorta. Note the curvature of the arch and the frequent branches (which are not drawn to scale). Flow enters from the heart through the aortic valve, which prevents much backflow.

a marked influence on the flow, and that it must ultimately be included in a theoretical analysis. Singh (1974) has examined steady entry flow in a uniform curved tube, and has shown how the secondary motions, which are a prominent feature of flow in curved tubes, are generated within the boundary layer. His analysis is valid only at distances from the inlet smaller than $(aR)^{\frac{1}{2}}$, where a is the tube radius ($\approx$ 0·8 cm in the dog) and R is the radius of curvature of the tube axis ($\approx$ 6 cm). Nevertheless it can be used to predict the quasi-steady flow which exists near the tube entrance when the flow as a whole is unsteady. As yet, however, the diffusive flow to which this must be matched downstream has not been calculated (this problem is currently being done).

(iv) *Velocity profile at the inlet.* We assume that the velocity profile is effectively flat, with an extremely thin boundary layer, at the downstream end of the aortic valve, which we call the inlet to the aorta. Bellhouse & Talbot (1969) found this to be true in experiments with model valves, and the animal experiments already quoted also indicate a fairly flat profile, although random disturbances are often superimposed on it, presumably originating in the left ventricle.

The blood velocity in the core of the ascending aorta varies with time in approximately the manner shown in figure 8. This curve has been constructed from a measured wave form given by Nerem *et al.* (1972), but some of the small pertur-

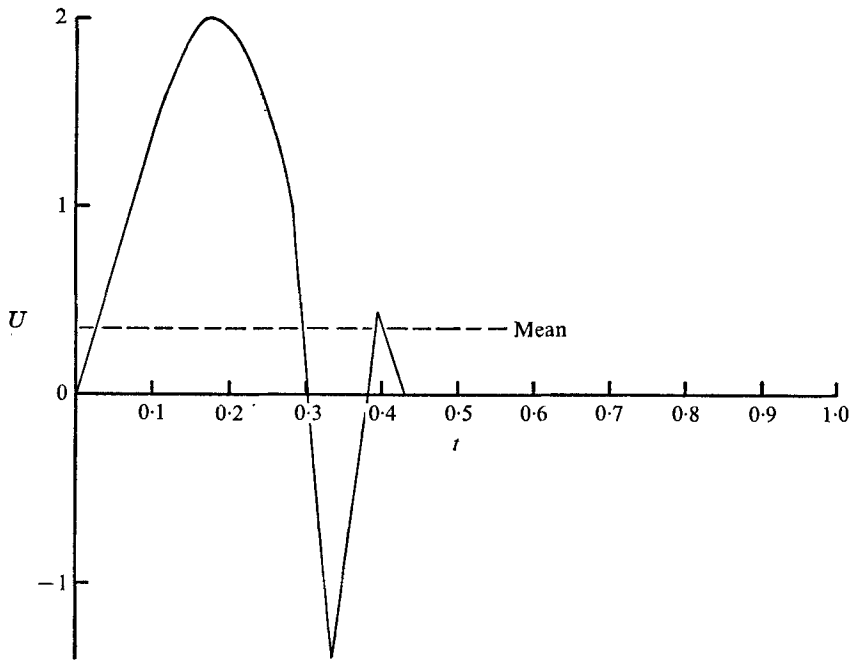

FIGURE 8. Dimensionless velocity $U(t)$ in the core of the aorta, simplified from a measured wave form given by Nerem *et al.* (1972). Note the sharp reversal as the aortic valve closes, and the fact that there is no core motion for over half the cycle. Peak velocity ($U = 2$) is 100 cm s^{-1}, mean velocity ($U = 0{\cdot}34$) is 17 cm s^{-1}; duration of beat ($t = 1$) is 0·4 s.

bations inevitably present *in vivo* have been smoothed out. In fact, this particular curve is made up of five straight lines and a segment of a sine wave, but it fits the data very well. The axes of the curve are dimensionless velocity U and time t. Since the tube is long, the non-dimensionalization of § 2 is inappropriate, and we have scaled the time with respect to the period of the cycle ($T = 0{\cdot}4$s) and the velocity with respect to half the peak velocity ($U_0 = 0{\cdot}5$ m s^{-1}). The mean dimensionless velocity is $\overline{U} = 0{\cdot}34$ (17% of the peak). The sharp reversal in velocity occurs when the aortic valve closes and bulges back into the ventricle because the pressure in the aorta briefly exceeds that in the ventricle.

The core velocity shown in figure 8 is zero for more than half the cycle. We assume that the fluid everywhere in the tube comes to rest by the end of the cycle, so that each beat can be treated as an isolated event, with the velocity initially zero. This cannot be entirely true, as we discuss below, but the predictions of unsteady wall shear will not be significantly affected by the small residual motions. The assumption is very useful, because it means that the thickness of the boundary layer which develops at the tube wall during every beat never exceeds a value of order $(\nu T)^{\frac{1}{2}}$. For blood in the dog aorta $(\nu T)^{\frac{1}{2}} \approx 0{\cdot}13$ cm, which is less than a tenth of the vessel diameter. Therefore we are justified in assuming (*a*) that acceleration of the core flow due to the displacement effect of the boundary layer is negligible, and (*b*) that the boundary layers on different

parts of the vessel circumference do not interact. We can therefore analyse the boundary layer as if it were on a semi-infinite flat plate, with the stream velocity as shown in figure 8.†

We are now in a position to apply the analysis of §2 directly. At each point on the tube wall, i.e. at each value of x (now non-dimensionalized with respect to $U_0 T$), the sequence of events is as follows. Initially there will be set up on the tube wall a diffusive (Rayleigh) layer, with the same thickness for all x, in which the velocity is given by (7) with $t_0 = 0$. A quasi-steady boundary layer will be initiated at the leading edge ($x = 0$), and will propagate downstream so that it takes over from the diffusive layer at a time t_{21} calculated from the relevant version of (10):

$$x = \int_0^{t_{21}} U(t)\,dt.$$

Then the (modified) quasi-steady solution will persist until after the time of peak forward velocity, $t = t_m$, and a new diffusive layer (not independent of x) will take over before the first flow reversal. Since the tube is long, no new quasi-steady layer can grow from the trailing edge, and the next quasi-steady layer to take over would do so during the second interval of forward flow. However, that can happen only at extremely small values of x, which we shall not consider. At less small values, the diffusive solution will persist until the end of the cycle ($t = 1$).

The quasi-steady regime around $t = t_m$ will not exist if the point x is too far from the leading edge for particles entering the tube at the start of the cycle to reach the point some time before t_m, and for particles entering it at t_m to reach the point before the first reversal. In the case considered here, no quasi-steady regime exists for $x > 0{\cdot}21$, i.e. for $\hat{x} > 4{\cdot}2$ cm, which is less than three vessel diameters from the entrance. For larger values of x, the diffusive solution (with $t_0 = 0$) exists throughout the cycle, and is the same for all x. This conclusion, however, leads to a contradiction, because if the flow is independent of x, the equation governing the velocity is linear. Hence the periodic function $U(t)$ can be split up by Fourier analysis into its mean and oscillatory components, and each analysed separately. The oscillatory components of u will represent Stokes layers, but the mean velocity field will be Poiseuille flow. Now the steady entrance length for Poiseuille flow is approximately $0{\cdot}03\,Re\,d$, where d is the vessel diameter and Re is the mean Reynolds number; in the present case this takes a value of about 33 cm, much greater than the 4·2 cm predicted above. So the flow cannot really be x-independent in the region between these two values of x. The error in the present method lies in neglecting the residual motions at the end of each cycle. After many cycles these would build up and the (x-dependent) mean flow be established. As we shall see, this neglect does not affect the predictions of oscillatory shear rate on the wall, but predictions of the mean shear rate will be in error, at least for $x > 0{\cdot}21$. Improved predictions for the wall

† The author is aware that, very near to the entrance of a tube, the displacement effect is considerable, and the inviscid flow in the core is not approximately parallel (Van Dyke 1970). However, this does not affect the first approximation to the flow in the boundary layer, and hence does not affect the wall shear.

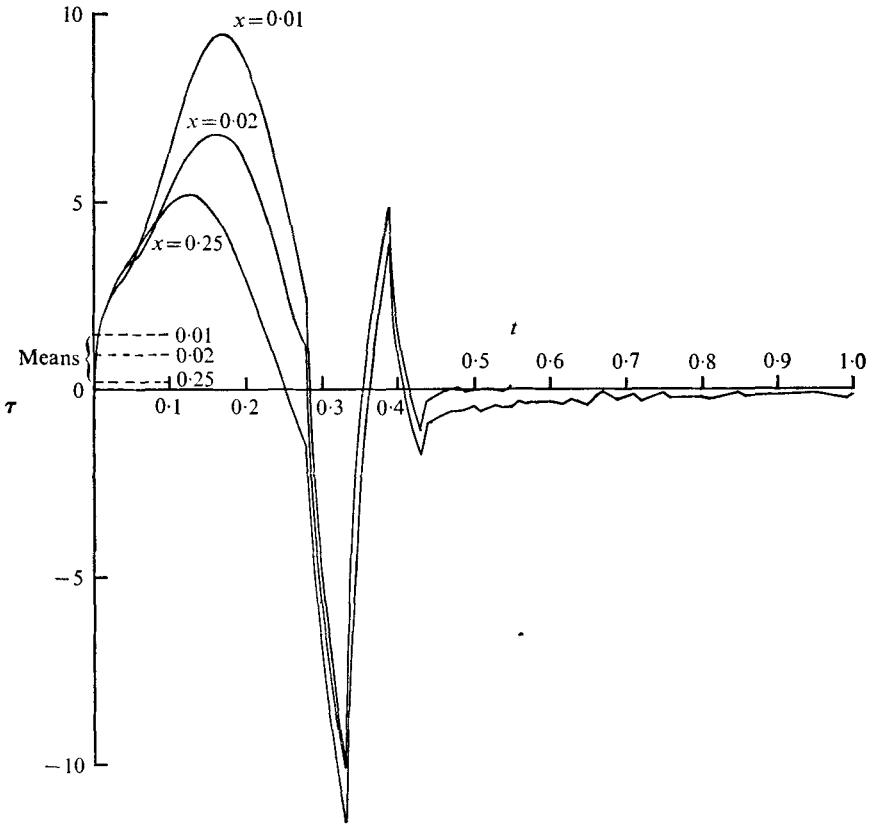

FIGURE 9. Dimensionless shear rate on the wall of the aorta, plotted against time, at three distances from the inlet. Motion in the boundary layer has almost completely died out by the end of the cycle.

shear downstream of $x = 0{\cdot}21$ can be achieved by an analysis like that of Pedley (1972*b*). Far downstream the developing mean boundary layer is independent of the oscillatory Stokes layer, and their interaction less far downstream can be analysed using the method of matched asymptotic expansions. Since we are here primarily interested in the oscillatory shear stress, we shall not investigate this region further.

The dimensionless wall shear rate τ is plotted as a function of time for three different values of x in figure 9. Very near the entrance ($x = 0{\cdot}01$) there is a large, quasi-steady peak in τ, almost in phase with the peak velocity. This diminishes rapidly as x increases, and has an increasing phase lead, which is to be expected as the modified quasi-steady boundary layer becomes thicker. However, at all times and at all values of x, the shear rates with the greatest magnitude are negative. These high reversed shear rates are a consequence of the large adverse pressure gradient associated with the rapid deceleration of the core flow as the aortic valve closes. It can also be seen that in all cases the wall shear has almost completely died away at the end of the beat, confirming that

the residual motions are very small, and can be neglected in calculations of the oscillatory components of wall shear.

The predicted values of the mean wall shear (which may be inaccurate, especially at the downstream site) are also shown in figure 9. At $x = 0{\cdot}01$, the mean is about 15% of the (negative) peak, compared with a mean velocity of 17% of the (positive) peak velocity. However, this falls rapidly, to about 2% of the peak, at values of x greater than 0·21, where the solution is diffusive all the time. The r.m.s. value of τ, on the other hand, falls from about 40% of the peak to about 30%, and remains considerably larger than the mean. In view of the large amplitude of the oscillations in τ, it seems much more likely *a priori* that the permeability of the artery wall, and thus the generation of atherosclerosis, is correlated with some measure of wall shear which is independent of direction, like the peak or r.m.s. value, rather than the arithmetic mean. Circumstantial evidence in support of this comes from the steady experiments by T. C. Carew, reported by Fry (1973), in which the rate of uptake of marked albumin into the wall of an excised segment of artery was found to be approximately proportional to τ^2, not τ.

Finally, we note that τ is non-dimensionalized with respect to $U_0(\nu T)^{-\frac{1}{2}}$, so in this case the peak wall shear rate is about 400 s^{-1}. This corresponds to a wall shear *stress* of 16 Nm^{-2}. Fry (1968) has demonstrated that the endothelium of an artery can be physically damaged by shear stresses in excess of 40 $N\,m^{-2}$. Such values are not achieved in this case, but they are not so far in excess of the prediction that the possibility of endothelial damage can be universally ruled out.

This work was supported by the Science Research Council.

REFERENCES

Atabek, H. B. & Chang, C. C. 1961 Oscillatory flow near the entry of a circular tube. *Z. angew. Math. Phys.* **12**, 185.

Bellhouse, B. J. & Talbot, L. 1969 The fluid mechanics of the aortic valve. *J. Fluid Mech.* **35**, 721.

Caro, C. G. 1973 Transport of material between blood and wall in arteries. In *CIBA Symp. Atherogenesis: Initiating Factors*, p. 127. Amsterdam: Assoc. Sci. Publ.

Caro, C. G., Fitz-Gerald, J. M. & Schroter, R. C. 1971 Atheroma and arterial wal shear. *Proc. Roy. Soc.* B **177**, 109.

Carrier, G. F. & DiPrima, R. C. 1956 On the unsteady motion of a viscous fluid past a semi-infinite flat plate. *J. Math. & Phys.* **35**, 359.

Clark, C. 1974 Thin film gauges for fluctuating velocity measurements in blood. *J. Phys.* E, *Sci. Instr.* **7**, 548.

Dennis, S. C. R. 1972 The motion of a viscous fluid past an impulsively started semi-infinite flat plate. *J. Inst. Math. Applic.* **10**, 105.

Fry, D. L. 1968 Acute vascular endothelial changes associated with increased blood velocity gradients. *Circulation Res.* **22**, 165.

Fry, D. L. 1973 Responses of the arterial wall to certain physical factors. In *CIBA Symp. Atherogenesis: Initiating Factors*, p. 93. Amsterdam: Assoc. Sci. Publ.

Hall, M. G. 1969 The boundary layer over an impulsively started flat plate. *Proc. Roy. Soc.* A **310**, 401.

LEWIS, J. A. & CARRIER, G. F. 1949 Some remarks on the flat plate boundary layer. *Quart. Appl. Math.* **7**, 228.

LIGHTHILL, M. J. 1975 *Mathematical Biofluiddynamics*. Philadelphia: SIAM.

MOORE, F. K. 1951 Unsteady laminar boundary layer flow. *N.A.C.A. Tech. Note*, no. 2471.

NEREM, R. M., SEED, W. A. & WOOD, N. B. 1972 An experimental study of the velocity distribution and transition to turbulence in the aorta. *J. Fluid Mech.* **52**, 137.

PEDLEY, T. J. 1972*a* On the forced heat transfer from a hot film embedded in the wall in two-dimensional unsteady flow. *J. Fluid Mech.* **55**, 329.

PEDLEY, T. J. 1972*b* Two-dimensional boundary layers in a free stream which oscillates without reversing. *J. Fluid Mech.* **55**, 359.

PEDLEY, T. J. 1975 A thermal boundary layer in a reversing flow. *J. Fluid Mech.* **67**, 209.

ROSENHEAD, L (ed.) 1963 *Laminar Boundary Layers*. Oxford University Press.

SEED, W. A. & WOOD, N. B. 1970 Use of a hot film velocity probe for cardiovascular studies. *J. Phys.* E, *Sci. Instr.* **3**, 377.

SINGH, M. P. 1974 Entry flow in a curved pipe. *J. Fluid Mech.* **65**, 517.

STEWARTSON, K. 1973 On the impulsive motion of a flat plate in a viscous fluid, II. *Quart. J. Mech. Appl. Math.* **26**, 143.

VAN DYKE, M. 1970 Entry flow in a channel. *J. Fluid Mech.* **44**, 813.

WHITMORE, R. L. 1968 *Rheology of the Circulation*. Pergamon.